On the performance of molecular polarization methods. I. Water and carbon tetrachloride close to a point charge

Marco Masia[a)]
Departament de Física i Enginyeria Nuclear, Universitat Politècnica de Catalunya, Campus Nord B4-B5, Barcelona 08034, Spain

Michael Probst[b)]
Institute of Ion Physics, Universität Innsbruck, Technikerstrasse 25, Innsbruck A-6020, Austria

Rossend Rey[c)]
Departament de Física i Enginyeria Nuclear, Universitat Politècnica de Catalunya, Campus Nord B4-B5, Barcelona 08034, Spain

(Received 6 July 2004; accepted 20 July 2004)

The three main methods to implement molecular polarization (point dipoles, fluctuating charges, and shell model) are tested against high level *ab initio* calculations for a molecule (water, carbon tetrachloride) close to a point charge (at the distance of a lithium or magnesium ion). The goal is to check whether an approximation (linear polarization) strictly valid at large intermolecular distances is sufficiently accurate for liquid state molecular dynamics simulations, where strong polarization effects are to be expected at short separations. The monitored observable is the molecular dipole moment as a function of the charge-molecule distance for selected molecular orientations. Analytic formulas are derived for the components of the molecular polarization tensor, facilitating the optimization of the performance for each polarization method as a function of its underlying parameters. Overall, the methods studied provide a remarkably good representation of the induced dipole, with no divergences appearing even at the shortest distances. For water close to a monovalent point charge the point dipole model, implemented with one or three dipoles, accurately reproduces the water dipole moment at all distances. Deficiencies appear as the molecular polarizability and/or charge increase: basically, the *ab initio* induced moments grow faster at intermediate distances than the linear increase characteristic of the phenomenological polarization methods, suggesting that nonlinear effects (hyperpolarizability) cannot be neglected in these cases. Regarding the capabilities of each method, the point dipole method is the one that performs best overall, with the shell model achieving acceptable results in most instances. The fluctuating charge method shows some noticeable limitations for implementations of comparable complexity (in terms of the number of sites required).
[DOI: 10.1063/1.1791637]

I. INTRODUCTION

It is widely accepted that the inclusion of polarization is indispensable for the next generation of molecular force fields in order to confidently simulate heterogeneous environments. Indeed, a substantial amount of work has already been directed towards this goal, mainly motivated by the accuracy required in biomolecular simulations[1,2] (as reflected, for instance, in the recent upgrading of the CHARMM force field with the inclusion of a fluctuating charge parametrization,[3] or an initial version of an atomic dipole model implemented in AMBER Ref. 4). At this point it might be convenient to critically examine the performance of the simple polarization methods that are being used, and the way in which polarizable force fields are constructed. In standard practice one of the available polarization methods is added to a force field functional (with, e.g., Lennard-Jones and Coulomb interactions) and parameters are optimized so that selected liquid state properties get acceptably close to experimental values or, in an alternative approach, to *ab initio* energies computed for several cluster configurations. Both methods share two basic problems related to the description of the electrostatic part: first, the performance of the polarization methods at short distances is seldomly addressed in detail (while there is no guarantee that they provide reasonable results in regions with highly nonhomogenous electric fields) and second, the electrostatic parameters get mixed with energetic or condensed phase properties, while this could in principle be avoided. An example should clarify these points: in the vast literature on ion solvation[5–27] (a scenario in which short range polarization effects can be expected to be particularly important) that makes use of classical polarizable methods, we are not aware of any work in which the induced dipole moment is computed as a function of the ion-molecule distance, and the results compared with *ab initio* calculations. Such a comparison might allow a reassessment of the way in which polarizability is handled

[a)]Electronic mail: marco.masia@upc.es
[b)]Electronic mail: michael.probst@uibk.ac.at
[c)]Electronic mail: rosendo.rey@upc.es

prior to the development of the force field. It is a test of this sort that will be undertaken here for the most popular polarization methods. Moreover, considering that high quality electrostatic multipoles are readily obtained in *ab initio* calculations, it is suggested that the electrostatic part might be decoupled from liquid state properties and/or cluster energies to better understand the effect of polarization. The contradictory results obtained to date on the contribution of molecular polarization might result from comparing force fields that have been optimized mixing electrostatic with energetic and/or condensed phase aspects in variable proportions, and using different polarization methods with uncontrolled or unclear behaviors at short distances.

As already emphasized, the environment of an ion in solution is of particular interest, which justifies to study polarization effects for ion-molecule dimers instead of, for instance, addressing molecules under strong homogeneous fields. Regarding the molecules selected, water is a mandatory choice. As stated, for instance, in a review by Elrod and Saykally,[28] many-body effects can have important manifestations in a number of bulk water properties and, unlike in most atomic and molecular systems, many-body effects in hydrated ion systems can result in substantial structural changes. Considering this critical role of water, it is remarkable that a simple and reliable polarizable model is not yet available although, starting with the pioneering work of Barnes *et al.*,[29] a large number of polarizable models have been developed in the past and new ones are being developed at an increasing pace[30–61] (the study of phase coexistence constitutes a relevant example of the difficulties encountered[62–64]). It is obvious that there is a need for such a model in order to replace the (nonpolarizable) workhorses of liquid state simulation (such as SPC/E Ref. 65 and TIP4P Ref. 66). Comparison with high level *ab initio* results for the dipole moment (or even higher multipoles) in strong nonhomogeneous electric fields (like those in the presence of an ion) might be a convenient and systematic way to guide future work. In this connection, only the work by Alfredsson *et al.*[67] on the water dimer, where polarization was modeled by a single point dipole and the most probable configurations were compared with *ab initio* calculations, is along the lines of what is reported here. Although different from the present approach, the concept of molecular polarization potential map has also been used to help understand the performance of different polarization models for the water molecule.[68] The main limitation of water, when looking for general guidelines, lies in its low polarizability. As an example of a highly polarizable molecule we selected carbon tetrachloride, which displays a number of interesting features: its polarizability is almost one order of magnitude larger than the one of water, it has no permanent dipole moment, and no polarization anisotropy.

Regarding the ions chosen, Li^+ should provide upper bounds on the polarization that a monovalent ion induces on neighboring molecules. Similarly, Mg^{++} is the smallest divalent ion of biochemical interest. It is important to keep in mind, though, that the present calculations correspond to a molecule in the vicinity of a point charge (singly or doubly charged), rather than to an actual lithium or magnesium ion. This is the case for both the *ab initio* results and for those with classical polarization methods (where only the molecule is allowed to be polarized). Although, in principle, there is no obstacle in computing the total induced dipole moment of an ion-molecule dimer (which will be addressed in a forthcoming contribution), several considerations justify this simplified approach. First, almost all simulation studies of solvated cations have neglected ion polarizability, so that it is important to assess to which extent these models hold when compared with *ab initio* calculations. An interesting issue is that of polarization divergence which has been often invoked to introduce damping schemes at short separations and ascribed to the use of point charge models. Although this claim has been disproved for the water dimer,[67] it might be possible that such divergence exists under the stronger fields created by small cations. Moreover, this simplified approach should provide a simple picture of molecular polarization, but one that can still be rigorously compared with *ab initio* results. Real ions would introduce a higher degree of complexity since the total polarization depends then on both ionic and molecular contributions as well as on charge transfer. Together with the fact that the total dipole moment for charged systems depends on an arbitrary origin, the result would not be intuitively clear. In short, the molecules have been treated exactly but for the ions it is assumed that beyond the ionic radius (our induced moments have only been computed down to the closest distance for the real ion-molecule dimer) they behave as point charges (this approximation is virtually exact from rather small separations onwards, as will be shown).

There are three approaches for the inclusion of polarization that are amply used,[2] and for which a comparative study is reported here: point dipoles,[69–71] electronic equalization (fluctuating charges),[72] and Drude oscillators or shell models.[73] Methods that handle many-body effects by including three-body terms (or higher) in the parametrization of energy,[74–76] without making use of explicit polarization, are also rather popular but are not included in the present study. While they have the advantage of computational efficiency and can accurately reproduce the energy landscape, they are unable to provide information on induced dipoles. We also do not analyze the extremely useful work on polarizable atoms designed to incorporate reaction fields into quantum chemical calculations.[77] Each of the methods studied here has, *a priori*, its strong and weak points. In the point dipole approach, the fact that dipoles are located on different sites substantially increases the complexity of molecular dyamics (MD) codes. This method, though, seems the most natural choice if a sort of hierarchical approach (feasible for increasing computational resources) is to be followed, since it would allow for the inclusion of higher multipoles.[78] The fluctuating charge method, in which site charges depend on the environment, is one of the most appealing because no significant changes need to be made in existing nonpolarizable codes. It has also the conceptional advantage to describe charge transfer within a molecule (on which this approach is based). Unfortunately, it is difficult to model out-of-plane dipole moments for planar molecules[43] or even polarizable atomic ions.[10] Finally, the shell model has similar advantages

regarding easiness of implementation. Its main problem might be the shortening of the time step that the inclusion of fast vibrating oscillators imposes and the use of more interaction sites. One important point that has not been addressed so far is that of the equivalence between these methods. In principle all three are capable of providing at least the same mean polarizability under homogeneous fields and are therefore indistinguishable at long intermolecular distances. However, at short separations it is not clear if they are still interchangeable, since they can (and do) have different responses to nonhomogeneous fields. While computational convenience has been a major factor to decide which method to use, it will be investigated here if this different performance at short distances could provide a physically based criterion. These methods do not encompass all the possibilities at hand. Mixed methods are also possible: within the fluctuating charge model, charges can be allowed to depart from their equilibrium positions[79] (i.e., an electronic equalization-Drude oscillator model), or, again using fluctuating charges, polarizable point dipoles can be added[53,80,81] (i.e., an electronic equalization-point dipole method). Obviously, any other combination is, in principle, possible. It is not clear, though, if these approaches can solve the problems of simple methods: if nonlinear effects turn out to be important (hyperpolarizability), none of these refinements would be capable of addressing them. This is one of the main focuses of the present work. Another reason not to address mixed methods at the outset is that simple methods have not been optimized in most cases; it suffices to say that we know of no simple polarizable model of water that displays the experimental anisotropic polarizability. Therefore we decided to investigate their maximum performance before embarking on more sophisticated approaches. To this end we have also derived analytic formulas for the polarization tensor components for each of the methods, since these are helpful in guiding the optimization process.

The outline of the paper is as follows: a summary of the polarization methods used is given in the following section. Details of the *ab initio* calculations for the chosen systems are summarized in Sec. III. The reader not interested in computational details can find the main results and the discussion of capabilities and shortcomings of each method in Sec. IV. The main conclusions are summarized in Sec. V.

II. POLARIZATION METHODS

Here we summarize the fundamentals of the polarization methods studied, together with the corresponding parameters for water and carbon tetrachloride required in each method. Moreover, analytic formulas are given for the polarization tensor in each case (with the mathematical derivation outlined in the Appendix for illustrative examples).

A. Fluctuating charges

In the chemical potential equalization method (CPE) Ref. 72 variable discrete charges are located on atomic sites within the molecule. Their value is computed, for a given molecular geometry, by minimization of the electrostatic energy. Within the context of liquid state simulations it is most usually known as the fluctuating charge method.[43]

For an isolated molecule, the molecular energy is expanded to second order in the partial charges

$$U_{\mathrm{molec}}=U_0(\{r\})+\sum_{i=1}^{M}\chi_i^0 q_i+\frac{1}{2}\sum_{i=1}^{M}J_i^0 q_i^2 + \frac{1}{2}\sum_{i=1}^{M}\sum_{j\neq i}^{M}J_{ij}(r_{ij})q_i q_j, \tag{1}$$

where $U_0(\{r\})$ denotes the charge independent contribution, χ_i^0 (''atomic electronegativity'') and J_i^0 (''atomic hardness'') are in principle characteristic of the atomic site i, and $J_{ij}(r_{ij})$ is a screening function, which is usually computed as the Coulomb integral of Slater ns atomic orbitals. In practice Eq. (1) is probably better regarded as a convenient expansion of the molecular energy, with parameters to be fitted from molecular properties, a perspective that will be exploited here to obtain the maximum possible performance of the method. Moreover, and although this possibility lies outside the scope of the present work, the $J_{ij}(r_{ij})$ coefficients are, in principle, dependent on the intramolecular distances if a flexible model is being considered (an Appendix in Ref. 82 contains a detailed discussion of how the calculation of intramolecular forces is affected in such case).

The CPE tenet is that atom electronegativities within the molecule ($\chi_i \equiv \partial U_{\mathrm{mol}}/\partial q_i$), should equalize ($\chi_1=\chi_2=\cdots\chi_M$), while maintaining overall neutrality ($\Sigma_{i=1}^{M} q_i=0$). This is equivalent to the minimization of the molecular energy with respect to the partial charges, again with the added condition of charge neutrality.

Particularizing to the case in which the molecule is subjected to an external homogeneous field, the total energy is given by

$$U=U_{\mathrm{molec}}-\vec{p}\cdot\vec{E}, \tag{2}$$

where $\vec{p}$ denotes the molecular dipole moment. If the energy is minimized, with the additional constraint of electroneutrality (with χ being the corresponding Lagrange multiplier),

$$\frac{\partial(U-\chi\Sigma_j q_j)}{\partial q_i}=0, \tag{3}$$

the following set of equations is obtained (with the first one applying for each site i within the molecule):

$$\chi_i+J_i^0 q_i+\sum_{j\neq i}J_{ij}q_j-\frac{\partial\vec{p}}{\partial q_i}\cdot\vec{E}=\chi, \tag{4}$$

$$\sum_j q_j=0, \tag{5}$$

from which the induced charges required to evaluate the molecular polarizability can be obtained.

We now give the analytic formulas for the polarization tensor components in the case of water and carbon tetrachloride. As a general rule, this tensor has no dependence on atomic electronegativities[83] (which are themselves linked to partial charges). This fact greatly facilitates the construction of fluctuating charge models: the J parameters can be optimized to reproduce the experimenal values of the polarization tensor components, while the electronegativities can be

TABLE I. Parameters for fluctuating charge models of water.

	SPC-FQ	TIP4P-FQ
d_{OH} (Å)	1.0	0.9572
d_{OM} (Å)	0.0	0.15
θ_{HOH} (deg)	109.47	104.52
J^0_{OO} (kJ mol^{-1} e^{-2})	1536.1	1555.3
J^0_{HH} (kJ mol^{-1} e^{-2})	1641.5	1477.5
J_{OH} (kJ mol^{-1} e^{-2})	1155.2	1198.7
J_{HH} (kJ mol^{-1} e^{-2})	820.4	852.2

tuned to reproduce any charge set of choice (often designed to reproduce multipole moments). Such approach has been successfully applied to neat carbon tetrachloride[84] and similar chloromethanes.[85]

1. Water

The most popular fluctuating charge models of water[43] consist of three charges, located, respectively, on the two hydrogen sites and on the oxygen (SPC-FQ) or an auxiliary site (M) on the molecular plane (along the line bisecting the bending angle and towards the hydrogens, TIP4P-FQ). Defining the z axis along the bisector of the bending angle and the x axis perpendicular to the molecular plane, the following expressions result[43] for the polarization components (see the Appendix):

$$\alpha_{xx}=0, \tag{6}$$

$$\alpha_{yy}=\frac{2d^2\sin^2(\theta/2)}{J^0_H-J_{HH}}, \tag{7}$$

$$\alpha_{zz}=\frac{2d^2\cos^2(\theta/2)}{J^0_H+J_{HH}-4J_{HO}+2J^0_O}, \tag{8}$$

where d denotes the oxygen-hydrogen (or M-hydrogen) distance and θ the angle between both bonds.

It is well known that neither of the models (SPC-FQ and TIP4P-FQ) does allow for induced dipoles perpendicular to the molecular plane (as reflected in the null value of α_{xx}). Within the present perspective, in which the emphasis is put on an accurate reproduction of induced moments, such behavior is regarded as an important flaw. Possible solutions involve an increase in the number of sites or the use of mixed methods (as discussed in the Introduction), and will not be pursued here. The required parameters for the SPC-FQ and TIP4P-FQ models[43] are summarized in Table I. The associated polarizabilities [obtained with Eqs. (6), (7), and (8)] are reported in Table II.

2. Carbon tetrachloride

In the case of carbon tetrachloride, with one fluctuating charge on each atomic site, all three polarization tensor components are equal,

$$\alpha_{CCl_4}=\frac{4d\cos[tg^{-1}(\sqrt{2})]}{J^0_{Cl}-J_{ClCl}}, \tag{9}$$

where d stands for the carbon-chloride distance and tetrahedral symmetry is assumed. It is important to note that as long as the difference $J^0_{Cl}-J_{ClCl}$ is kept constant, the same molecular polarizability is obtained. Therefore the J values can be optimized so that the best possible accord for induced dipole moments at short distances is obtained (it is also interesting to note that the carbon hardness does not contribute to the molecular polarizability). Subsequently, only the results with the model used by Llanta and Rey[84] to study induced absorption in liquid carbon tetrachloride will be reported since, as will be shown within, no significant improvement [based on Eq. (9)] is possible. The corresponding parameters are[84] $J^0_C=962.259$ kJ/(mol e^2), $J^0_{Cl}=983.844$ kJ/(mol e^2), $J_{CCl}=577.796$ kJ/(mol e^2), $J_{ClCl}=432.919$ kJ/(mol e^2), and $d=1.766$ Å, which reproduce the experimental polarizability (10.5 Å^3) when inserted in Eq. (9).

B. Point dipoles

In this method both fixed partial charges and induced dipoles are located within the molecule. The value of the induced dipoles ($\vec{p}_i$) can be derived starting from the electrostatic energy of a polarizable particle (of polarizability α_i) subject to an external field[86,87]

$$U_i=-\vec{p}_i\cdot\vec{E}_i+\frac{p_i^2}{2\alpha_i}, \tag{10}$$

where $\vec{p}_i$ denotes the induced dipole.

The field is produced by the external partial charges ($\vec{E}^0$) and by both the intramolecular and external induced dipole moments

$$\vec{E}_i=\vec{E}^0_i+\sum_{j\neq i}T_{ij}\cdot\vec{p}_i, \tag{11}$$

where T_{ij} denotes the dipole field tensor

$$T_{ij}=\frac{1}{r_{ij}^3}\left[3\frac{\vec{r}_{ij}\vec{r}_{ij}}{r_{ij}^2}-I\right]. \tag{12}$$

The following expression results for the electrostatic energy associated to induced dipoles:

TABLE II. Experimental polarizabilities of water compared to those corresponding to the different classical models studied.

	SPC-FQ	TIP4P-FQ	PSPC	POL1	RPOL	PDM	RER	PD1-H2O	PD2-H2O	Expt.
$\bar{\alpha}$ (Å^3)	1.09	1.12	1.44	0.979	1.975	1.44	1.44	1.47	1.47	1.47
α_{xx} (Å^3)	0.0	0.0	1.44	0.922	0.933	1.44	1.44	1.428	1.415	1.415
α_{yy} (Å^3)	2.26	2.55	1.44	1.464	3.759	1.44	1.44	1.532	1.528	1.528
α_{zz} (Å^3)	1.02	0.82	1.44	0.550	1.234	1.44	1.44	1.451	1.468	1.468

TABLE III. Parameters for point dipole models of water.

	PSPC	POL1	RPOL	PDM	RER	PD1-H2O	PD2-H2O
d_{OH} (Å)	1.0	1.0	1.0	0.9572	0.9572	0.9572	0.9572
d_{OM} (Å)	0.0	0.0	0.0	0.215	0.15	0.22	0.0606
θ_{HOH} (deg)	109.47	109.47	109.47	104.52	104.52	104.52	104.52
α_O (Å^3)	1.44	0.465	0.528	0.0	1.44	0.0	0.0
α_M (Å^3)	0.0	0.0	0.0	1.444	0.0	1.420 48	1.4099
α_H (Å^3)	0.0	0.135	0.170	0.0	0.0	0.001 92	0.0038

$$U_p = -\frac{1}{2}\sum_i \sum_{j\neq i} \vec{p}_i \cdot T_{ij} \cdot \vec{p}_j - \sum_i \vec{p}_i \cdot \vec{E}_i^0 + \sum_i \frac{p_i^2}{2\alpha_i}, \quad (13)$$

which, if minimized with respect to $\vec{p}_i$, yields an implicit expression for the induced dipole

$$\vec{p}_i = \alpha_i \left[\vec{E}_i^0 + \sum_{j\neq i} T_{ij} \cdot \vec{p}_j \right], \quad (14)$$

which can be solved iteratively in numerical simulations.

Since interactions are allowed between induced dipole moments located on different sites within a molecule, the present model has a nonadditive character. Consistent sets of nonadditive atomic polarizabilities have been derived that allow to satisfactorily reproduce the molecular polarizabilities of different molecular families.[69] According to our knowledge no analytic formulas are available in the literature for the polarization tensor principal components for polyatomic molecules, not even in the very important case of water.

1. Water

Adopting the same geometrical definitions as for the fluctuating charge model, the following expression results for the polarizability along the z axis (see the Appendix):

$$\alpha_{zz} = (\alpha_O + 2\alpha_H) + \frac{16\alpha_O^2\alpha_H \sin^3(\theta) - 32\alpha_O\alpha_H d^3 \sin^3(\theta) + 32\alpha_O\alpha_H^2 \sin^3(\theta) - 2\alpha_H^2 d^3}{8d^6 \sin^3(\theta) - 16\alpha_O\alpha_H \sin^3(\theta) + \alpha_H d^3}. \quad (15)$$

The terms within the first parenthesis correspond to the result that would be obtained if the model had an additive character (in this limit different additive atomic polarizabilities should be used, which are also available[69]). The somewhat involved last term thus represents the effect of intramolecular interactions between induced dipoles. We have not attempted to partition the polarization tensor component in a similar way for the two other cases, in order to avoid unnecessarily increasing the complexity of the formulas.

$$\alpha_{yy} = \frac{\alpha_O\left(1 - \frac{\alpha_H}{4d^3\sin^3(\theta)}\right) + 2\frac{\alpha_H\alpha_O[3\sin^2(\theta)-1]}{d^3} + 2\alpha_H\left(1 - 144\frac{\alpha_O\alpha_H\sin^5(\theta)\cos^2(\theta)}{8d^6\sin^3(\theta) - \alpha_H d^3}\right) + 2\frac{\alpha_O\alpha_H[3\sin^3(\theta)-1]}{d^3}}{\left(1 - 144\frac{\alpha_O\alpha_H\sin^5(\theta)\cos^2(\theta)}{8d^6\sin^3(\theta) - \alpha_H d^3}\right)\left(1 - \frac{\alpha_H}{4d^3\sin^3(\theta)}\right) - 2\frac{\alpha_O[3\sin^2(\theta)-1]\alpha_H[3\sin^3(\theta)-1]}{d^6}}, \quad (16)$$

$$\alpha_{xx} = \frac{\alpha_O\left(1 + \frac{\alpha_H}{8d^3\sin^3(\theta)}\right) + 2\frac{\alpha_H\alpha_O[3\cos^2(\theta)-1]}{d^3} + 2\alpha_H\left(1 - 72\frac{\alpha_O\alpha_H\sin^5(\theta)\cos^2(\theta)}{4d^6\sin^3(\theta) + \alpha_H d^3}\right) + \frac{2\alpha_O\alpha_H[3\cos^3(\theta)-1]}{d^3}}{\left(1 - 72\frac{\alpha_O\alpha_H\sin^5(\theta)\cos^2(\theta)}{4d^6\sin^3(\theta) + \alpha_H d^3}\right)\left(1 + \frac{\alpha_H}{8d^3\sin^3(\theta)}\right) - 2\frac{\alpha_O[3\cos^2(\theta)-1]\alpha_H[3\cos^3(\theta)-1]}{d^6}}. \quad (17)$$

A large number of models exist for water, ranging from those with only one point dipole (located on the oxygen or on the M site) to those that have three point dipoles, respectively, located on the hydrogens and, again, on the oxygen or M sites. A summary of the parameters for each of the models studied here is given in Table III (although only the most successful will be discussed). The associated polarizabilities, obtained with Eqs. (15)–(17) for the cases with three point dipoles, are reported in Table II. It should be noted that models with only one dipole are isotropic, while the water molecule displays anisotropic polarizabilities. Although this is, in principle, a reasonable approximation (the difference between polarization tensor components is less than 10%), it is not clear to what extent it can be trusted at short distances, a point that will be addressed here. It is somewhat surprising that none of the models with three point dipoles available in

TABLE IV. Site polarizabilities for the different CCl_4 point dipole methods discussed.

	Reference 69	PD-CCl4	PD-central
α_C (Å^3)	0.878	−1.000	10.51
α_{Cl} (Å^3)	1.910	2.880	0.00

the literature have aimed to reproduce the experimental anisotropic components, while an excellent match can be attained by optimizing the oxygen (or *M* site) and hydrogen polarizabilities with the help of Eqs. (15)–(17). The result of such optimization is denoted PD1-H2O in Table III (there the charge is located on the *M* site characteristic of the TIP4P model, as this turns out to be superior to locating it on the oxygen). We have also included the position of *M* in the optimization process, and denoted the resulting model PD2-H2O; it reproduces correctly the (gas phase) experimental anisotropic polarizabilities (see Table II).

2. Carbon tetrachloride

If induced dipoles are located on each atomic site and tetrahedral symmetry is assumed the following expression is obtained:

$$\alpha_{CCl_4}=(\alpha_C+4\alpha_{Cl})+\left(4\sqrt{2}\alpha_C+\frac{9\sqrt{3}}{8}\alpha_{Cl}\right)\frac{2048\alpha_C\alpha_{Cl}+288\sqrt{2}\alpha_{Cl}^2}{1024\sqrt{2}d^6-8192\sqrt{2}\alpha_{Cl}\alpha_C-243\sqrt{2}\alpha_{Cl}^2+96\sqrt{3}\alpha_{Cl}d^3}. \tag{18}$$

Similar to the case of fluctuating charges, the molecular polarizability (α_{CCl}) depends on two parameters (α_C,α_{Cl}), so that an infinite number of pairs can be obtained that yield the same molecular polarizability. Again, this feature has been exploited to explore the maximum performance of the method. Results for two different sets are reported (Table IV): the model proposed in Ref. 69, and an optimized point dipole model (PD-CCl4) developed here along the lines just described.

C. Shell model

Several denominations (Drude oscillator, charge-on-spring, shell model) exist for closely related versions of this method. Essentially, induction is represented by charged particles attached by springs to several sites within the molecule. In its most simple (albeit rather popular) form only one charge is used which, for instance in the case of water, might be attached to the oxygen site. Under the effect of an external field the position of each auxiliary charge is adjusted to minimize the electrostatic energy.

The total partial charge for each site (q_i) is split between a fixed charge (q_i-q_{Di}) and an auxiliary charge (q_{Di}) that is allowed to move in the vicinity of the site (so that in absence of external field, both charges will overlap, with a net charge q_i). Note that, in the present formulation, this is an additive model since no intramolecular interactions are considered between charges, the displacement of auxiliary charges stems from external fields only. Each auxiliary charge is harmonically bound to its site (with position vector $\vec{r}_i$) by a spring of force constant k_i. Under the effect of the external field it will settle on an equilibrium position $\vec{r}_i+\vec{d}_i$. The part of the total energy associated to the induced dipoles generated when the molecule is under the effect of an external field is given by

$$U=\sum_i \tfrac{1}{2}k_i d_i^2-\sum_i \vec{p}_i\cdot\vec{E}, \tag{19}$$

where the first term stands for the energy of the oscillators and the second for that of the induced dipoles in the presence of the external field.

The equilibrium position will be found by solving

$$\frac{\partial U}{\partial \vec{d}_i}=0, \tag{20}$$

which, considering that $\vec{p}_i=\Sigma_i q_{Di}\vec{d}_i$, yields

$$k_i\vec{d}_i-q_{Di}\vec{E}=0 \tag{21}$$

so that

$$\vec{d}_i=\frac{q_{Di}}{k_i}\vec{E}. \tag{22}$$

Inserting into the formula for the induced dipoles, we get

$$\vec{p}_i=\sum_i \frac{q_{Di}^2}{k_i}\vec{E}, \tag{23}$$

from which the polarizability in the direction of $\vec{E}$ is identified as

$$\alpha=\sum_i \frac{q_{Di}^2}{k_i}. \tag{24}$$

Since the result is independent of the electric field direction, an important limitation is that molecular polarization in this method is isotropic (even if more than one site per molecule is used). Regarding parameter optimization, somewhat different approaches are possible. In principle each term of the sum could be identified with the corresponding atomic polarizability ($\alpha_i\equiv q_{Di}^2/k_i$), which makes more evident the additive nature of the model [as Eq. (24) reduces to $\alpha=\Sigma_i\alpha_i$]. If these atomic polarizabilities are taken as given[69] then only one free parameter is left for each site (q_{Di}^2 or k_i). In another approach, since the (average) molecular polarizability is the only observable atomic polarizabilities are used as first guess of the quotients (q_{Di}^2/k_i), but all param-

TABLE V. Parameters for shell models of water.

	Reference 56	Reference 58	Reference 76	SH-H2O
d_{OH} (Å)	1.0	1.0	1.0	0.9572
d_{OM} (Å)	0.0	0.0	0.0	0.215
θ_{HOH} (deg)	109.47	109.47	109.47	104.52
k_O (kJ mol^{-1} Å^2)	61 535.44	4185.5	65 784.0	0.0
k_M (kJ mol^{-1} Å^2)	0.0	0.0	0.0	62 597.64
k_H (kJ mol^{-1} Å^2)	0.0	0.0	4597.0	29 096.44
$q_{DO}(e)$	−8	2.082 41	−5.00	0.0
$q_{DM}(e)$	0.0	0.0	0.0	8.0
$q_{DH}(e)$	0.0	0.0	−0.75	0.2

eters are subsequently varied (with the only restriction that the total molecular polarizability remains unchanged). Both approaches have been followed here in order to explore the maximum performance of the method. Actually, numerical efficiency also puts an important restriction on the sort of models that are acceptable. Since in its most popular form the method is applied making use of a generalized Lagrangian, with the dynamics of the auxiliary sites integrated together with that of the nuclei, spring stiffness cannot be too large since this would require a rather short time step. Conversely, the charges cannot be large either, with $\approx 10e$ being a rough upper bound of the values that can be found in the literature.

Parameters for the different models available for water, and for the optimized one developed in this work (SH-H2O), are summarized in Table V. The corresponding polarizabilities can be found in Table II. For carbon tetrachloride there are no available models, an optimized version has been developed here (SH-CCl4 with parameters $k_C=0.0$, $q_{DC}=0.0$, $k_{Cl}=13\,206\,\mathrm{kJ\,mol^{-1}\,Å^2}$, $q_{DCl}=5e$), which yields the experimental polarizability.

III. *AB INITIO* CALCULATIONS

The performance of the polarization models discussed in this work is examined by comparing the induced dipole moments with those from *ab initio* calculations on the same systems. Therefore it must be ensured that the reference calculations are of sufficient accuracy. From a quantum chemical viewpoint, electrostatic properties such as induced dipole moments (and polarizabilities) are one-electron properties or properties of the (linear response of the) ground-state electron density and can be calculated semiquantitatively already on the Hartree-Fock level if sufficiently flexible basis sets are used. Qualitatively wrong Hartree-Fock dipole moments[88] are found for small dipole moments, however, and accurate calculations of these properties require inclusion of electron correlation. For polarizabilities, Hartree-Fock calculations underestimate polarizabilities typically by up to 10%. The low accuracy of Hartree-Fock calculations with respect to polarizability calculations is also evident from the well-known approximate character of Koopmans' theorem since, to the first-order of perturbation theory, the polarizability is proportional to the sum of the reciprocal excitation energies [$\alpha \approx 1/(E_0-E_n)$; E_n is the nth excited state]. Just opposite to Hartree-Fock, density functional calculations with simple functionals (VWN Ref. 89, BLYP Ref. 90) overestimate polarizabilities. Newer density functionals such as B3LYP Ref. 91 perform better[92] and give an error around 2%[93] or less[94] if used with specially designed basis sets.[95] For our calculations we decided to use the B3LYP density functional with the aug-cc-pVTZ Ref. 96 basis set since a vast number of studies have already demonstrated its accuracy also for other quantities we are interested in with respect to future investigations. A good overview of the performance of density functionals for the calculation of electrical properties is given in Ref. 97.

In order to find the minimum of the potential energy curves Li^+ and Mg^{2+} were described with the 6-311G* basis set[98] since for these metals no aug-cc-pVTZ basis is available. Then the potential curves were calculated by moving the ions in the directions relative to H_2O and CCl_4 described in the subsequent sections. The curves of the induced dipole moments as function of the distance were calculated in the same way except that the ions are replaced by point charges without basis functions.

IV. MOLECULE CLOSE TO MONOVALUED CHARGE

We first address molecular polarization in the proximity of a monovalued charge with the radius of a lithium cation.

A. Water

The performance of molecular polarization methods only needs to be studied for distances that are physically relevant, so we start by estimating the distance of closest approach. Figure 1 displays the Li^+-H_2O energy profiles computed *ab initio* for several molecular orientations (full lines). The same calculation has been performed for a point charge (dashed lines) instead of a lithium ion in order to ascertain from which separation the approximation used here for the ion is accurate. Five molecular orientations have been selected: C_{2v}-*face*, with the molecular dipole pointing away from the ion, corresponds to the most probable orientation in the vicinity of a cation, as reflected in the deeper minimum; *trans* corresponds to a similar configuration with the molecule slightly tilted, so that there is a collinear ion-oxygen-hydrogen arrangement; *top* is a rather different geometric configuration which remarkably has almost the same energy profile as *trans*, and in which the ion approaches the water molecule perpendicular to the molecular plane and towards the oxygen; C_{2v}-*back* and *cis* have been included for completness, since they have dissociative profiles and therefore will be rather unprobable; in C_{2v}-*back* the water molecule

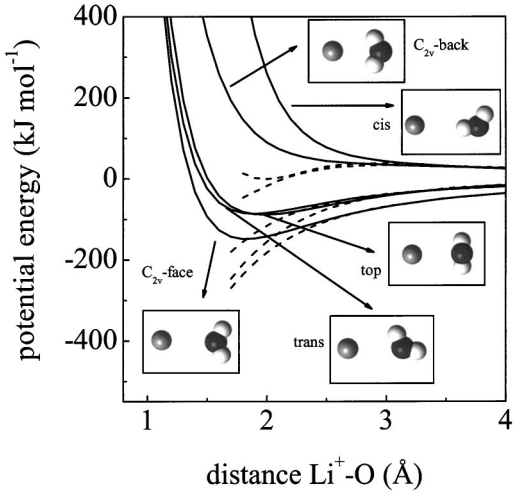

FIG. 1. *Ab initio* potential energy curves for Li^+-H_2O (solid lines) and for (+)-H_2O (dashed lines).

has been inverted with respect to C_{2v}-*face* and in *cis* the water molecule has been inverted with respect to *trans*. The distance of maximum approach has been determined in each case as that in which the interaction energy is $\approx 10k_BT$, which guarantees that no shorter distances will be reached during a typical liquid state simulation. This criterion results in a "radius" slightly smaller than 1.5 Å for C_{2v}-*face*, *trans*, and *top* configurations, which seems a safe estimation since it is substantially smaller than the shortest distances found (≈1.7 Å) in molecular dynamics simulations of Li^+ in water for a broad range of thermodynamic conditions[99] (using an effective potential). This minimal distance for C_{2v}-*back* and *cis* was chosen to be 4 Å. Compared with a real cation, the point charge approximation is virtually exact down to 3 Å for C_{2v}-*back* and *cis* (the distance at which the solid and dashed lines start to diverge), and down to 2.5 Å for C_{2v}-*face*, *trans*, and *top*. These values can be taken as indicative of the closest distances where the induced dipole moments computed here faithfully represent those of the real ion-molecule dimer.

The first five panels in Fig. 2 display the modulus of the total dipole moment of the water molecule for each of the chosen orientations (the last panel displays the *x* component of the induced dipole moment for the *top* configuration). In each case, the results are shown only for the physically relevant range (see above). Vertical dashed lines indicate the distance at which the potential energy profiles obtained for the ion or for a point charge are still indistinguishable. Each

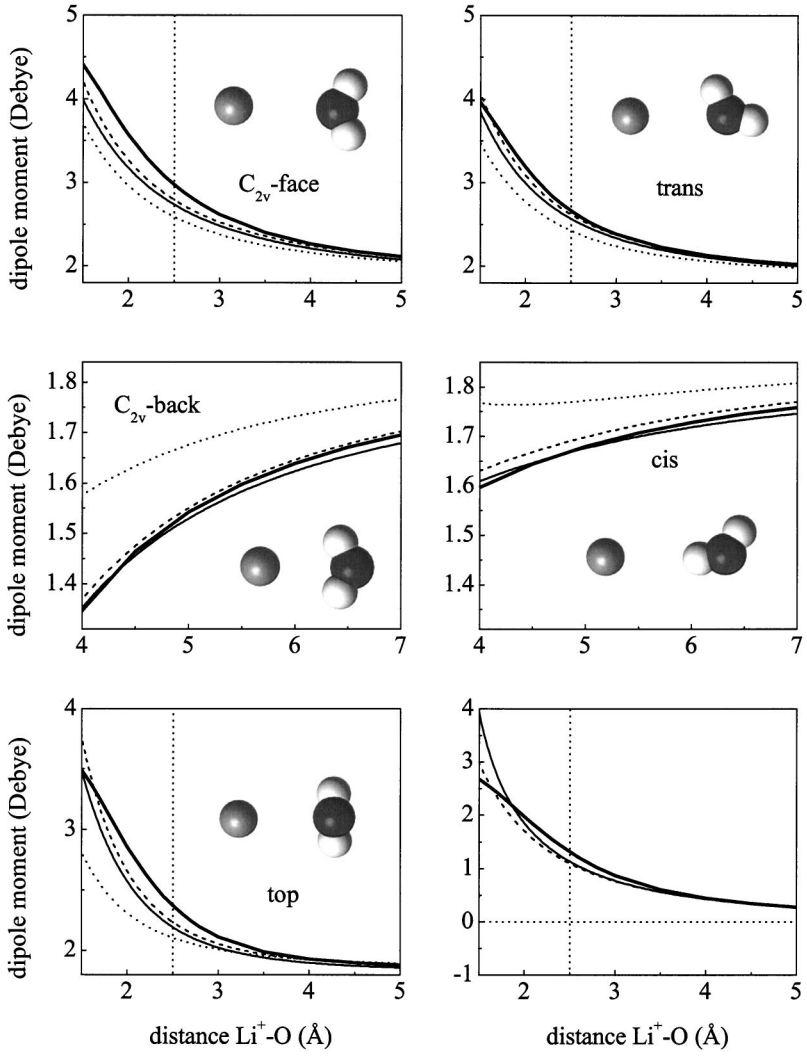

FIG. 2. Water-monovalued charge: total dipole moments for representative configurations (sketched in the insets). *Ab initio* (thick solid line), shell model (thin solid line), point dipoles (dashed line), fluctuating charges (dotted line). The last panel displays the *x* component of the induced dipole moment for the *top* configuration. Vertical dashed lines indicate the distance at which the point charge model of the ion is still accurate for the potential energy.

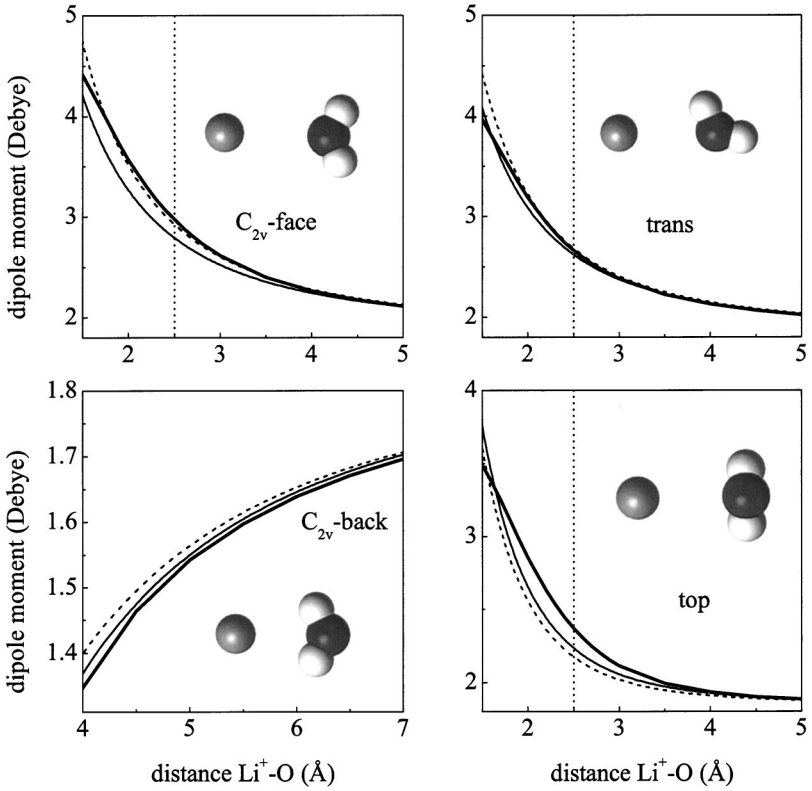

FIG. 3. Water-monovalued charge: comparison of the best results using point dipoles. *Ab initio* (thick solid line), PDM (thin solid line), and PD2-H2O (dashed line).

plot includes the *ab initio* result together with the best point dipole, shell, and fluctuating charge models. Before discussing each one in turn, several things can be observed at the outset. First, inspection of the shortest distances shows that induced dipoles can substantially exceed the permanent dipole moment (1.85 D) (with total dipole moments that reach up to 4.5 D for the most probable orientation, i.e., an induced dipole of 2.65 D), which highlights the importance of including polarization in order to properly describe these strong induction effects. Conversely, inspection at larger distances shows that all methods are interchangeable from a distance of 4–5 Å (i.e., two molecular diameters), which signals the distance from which the linear polarizability approximation is virtually exact. Regarding the performance of each method, the shell and point dipole method reproduce fairly well the *ab initio* profiles, the latter method coming even closer at the shortest distances. Finally, another important conclusion can be drawn: when compared with the *ab initio* results, no overestimations are observed for any of the polarization methods. This is in line with the conclusion obtained for water dimers,[67] according to which the high dipole moments obtained in molecular dynamics simulations of polarizable water using the point dipole approximation cannot be ascribed to a failure of the method. Actually, this notion is considerably reinforced here since it is tested close to a monovalent ion for several polarization methods. If any, the only noticeable deviation goes in the opposite direction and is to be found at intermediate distances (2–3 Å), for which the *ab initio* results predict slightly higher induced dipoles than those obtained with the phenomenological methods. This discrepancy will be shown to be stronger for higher ionic charge or molecular polarizability, and is thus ascribed to nonlinear polarization (not reproducible by the classical methods tested here), which in this case is only barely noticeable. Finally, concerning the validity of the present results for a real ion-molecule dimer, all the above conclusions are equally valid for distances larger than those indicated by the vertical dashed lines.

We now turn to a case per case analysis of each polarization method, although given the large number of models studied, only the main aspects will be included (for the best models). The point dipole models can be classified in two distinct groups: those with one point dipole and those with three dipoles. Within the first group the differences lie in the position of the dipole. Several possibilities have been tried: the oxygen site,[30,40] the center of mass.[29,47] and finally, those that locate it on the *M* site,[48] with oxygen-*M* distances that can be varied.[67] From the comparison (not included) of all these models, and again in line with the results for the water dimer,[67] the best accord with the *ab initio* profiles is obtained when the point dipole is located on an *M* site, with a distance of $\approx$0.2 Å from the oxygen. Therefore the single-dipole models reported in Ref. 48 and (the best model) in Ref. 67 provide an optimal representation of the molecular induced dipole on the water molecule (and will be denoted PDM). Actually, a single point dipole model is optimal since none of the models with three point dipoles that have been tried is able to outperform it. A comparison between the best one-dipole and three-dipoles models, for a selected number of orientations, is displayed in Fig. 3. Several three point models have been tried (with parameters summarized in Table III), which include two new optimized models (PD1-H2O and PD2-H2O, described in Sec. II B 1). The best model with three dipoles is PD2-H2O, and although its description of the

induced dipole is excellent in all cases (Fig. 3), it is still slightly worse than a one-dipole model at contact. This is good news from the simulation point of view since there is no need to include more than one dipole per molecule, although it is somewhat surprising given that PD2-H2O displays the exact experimental anisotropic polarizabilities (see Table II) in contrast with the isotropic polarizabilitiy of a one-dipole model.

Regarding the shell model, the best implementation is the one optimized here (SH-H2O, see Table V and Table II), and displayed in Fig. 2. As stated above its performance is excellent, although it slightly overestimates the induced dipoles at contact, particularly for the *top* configuration (although it is important to recall that such close separations are not observed in MD simulations). The result that a method without anisotropic polarizabilities displays such a good agreement is in line with the results obtained with the point dipole method, according to which a one-dipole (isotropic) model is excellent. In this case, contrary to what has been observed for point dipoles, the shell model performs better if the polarizability on hydrogens is included.

Finally, both fluctuating charge models are clearly inferior to optimized shell or point dipole models for all configurations, as can be seen in Fig. 2 (where only the best one, SPC-FQ, is displayed). It is known that the main failure is to be expected for the *top* configuration, as displayed in the sixth panel of Fig. 2. There, instead of the total dipole moment, only the component of the induced dipole moment along the *x* axis is plotted (flat dashed line), showing that the fluctuating charge model yields a null induced dipole perpendicular to the molecular plane, while the other two methods predict the right *ab initio* result at all distances. Again, as for the other orientations, this induced dipole is substantial (up to 2.5 D) and certainly cannot be considered a small discrepancy. However, the fluctuating charge model can predict part of the *total* dipole in the *top* configuration (ion perpendicular to the molecular plane), since such configuration also induces some polarization on the molecular plane due to the hydrogen sites polarizability (fifth panel in Fig. 2). Moreover, in all other configurations (first four panels in Fig. 2) the fluctuacting charge models underestimate the induced dipole moment as well, which is consistent with the fact that both have a mean molecular polarizability which is ≈20% lower than the experimental one. This underestimation is not only due to neglecting the perpendicular component but also due to a low in-plane polarizability along the direction perpendicular to the molecular dipole (*y* axis), which is roughly half of the experimental value. It is also the case that the polarizability along the dipole axis (*z*) is substantially higher than the experimental one. While it would be relatively easy to get the correct experimental polarizabilities along the *y* and *z* axis by optimizing the parameters in Eqs. (7) and (8), the fact that no improvement is possible for the *x* axis precludes this option. It is obvious that a higher number of sites is required for a real improvement (or the use of a mixed model) with the consequent computational burden in MD simulations, and that this is probably not worth being pursued given the success of, for instance, point dipole models with only one dipole.

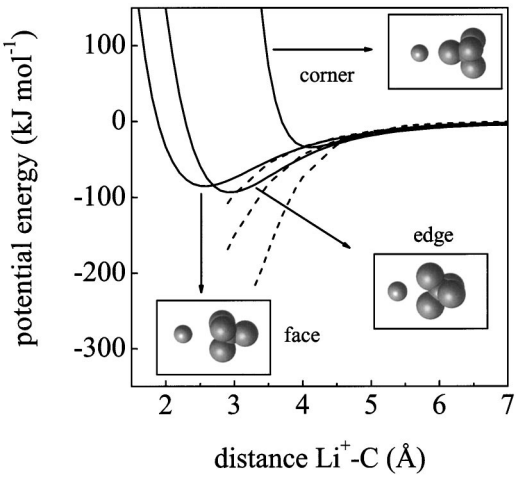

FIG. 4. *Ab initio* potential energy curves for Li^+-CCl_4 (solid lines) and for (+)-CCl_4 (dashed lines).

B. Carbon tetrachloride

Its much higher polarizability (10.5 Å^3 compared with 1.4 Å^3 for water) together with its spherically symmetric polarizability, makes this molecule an ideal case to study the limits of some of the conclusions drawn from water. Figure 4 displays the Li^+-CCl_4 energy profiles computed for several molecular orientations (full lines), together with the corresponding profiles for the point charge approximation (dashed lines). Three molecular orientations have been studied (with sketches included in Fig. 5), with two of them being almost equally stable (as shown in Fig. 4): in the *face* configuration the ion occupies a position above the center of the triangle defined by three chlorine atoms and its minimum occurs at the shortest distance (≈2.5 Å), in the *edge* configuration the ion sits above the line between two chlorine atoms with the minimum at a somewhat larger distance (≈3 Å). It is noteworthy that the well depth in both cases is not far from that of the water dimer (see Fig. 1), showing that electrostatic interactions due to induced dipoles are not *per se* weaker than interaction energies from permanent ones (a phenomenon that is known to occur in other cases, see Sec. 15 in Ref. 86). Finally, for the *corner* configuration, with a collinear ion-chlorine-carbon alignment, the well is shallower and occurs at a larger distance (≈4 Å). Concerning the accuracy of the point charge approximation for the ion, it is virtually exact down to 4.5 Å for the *corner* configuration and down to 3.5 Å for the *face* and *edge* orientations. The distance of maximum approach is ≈1.8 Å for the *face* configuration, ≈2.2 Å for edge, and ≈3.6 Å for *corner* (note the different origins of the horizontal axis in Fig. 5).

The results from several models are displayed in Fig. 5. We first note that the *ab initio* calculations predict rather high induced dipole moments (of up to 8 D for the *corner* configuration), much larger than those of the water molecule, and roughly one order of magnitude larger than those in neat liquid CCl_4 (which have a mean value of 0.19 D and a maximum value of ≈0.7 D, see Ref. 84). From the preceding analysis of the water molecule and the spherical symmetry of CCl_4, one may think that only one point dipole (with the

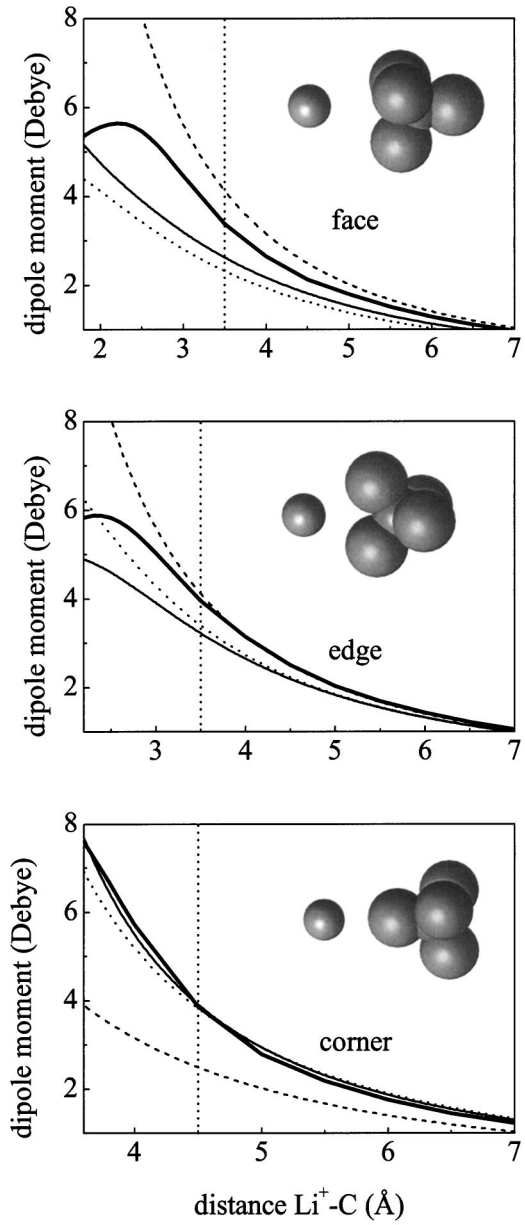

FIG. 5. CCl_4-monovalued charge: total dipole moments for representative configurations. *Ab initio* (thick solid line), point dipole of Ref. 69 (thin solid line), PD-central (dashed line), and fluctuating charges (dotted line). Vertical dashed lines indicate the distance at which the point charge model of the ion is still accurate.

molecular polarizability located on the carbon site) might be adequate. Indeed, this model is fairly reasonable for distances for which the point charge approximation for the ion is accurate (vertical dashed lines). However, and as displayed in Fig. 5, such model would produce strong divergences at short distances, particularly for the most stable configuration (*face*). For this orientation the single point dipole model overestimates the induced dipole for all distances. Therefore, the optimal model for water performs rather poorly for carbon tetrachloride, indicating that the selection of a model should be decided on a case per case basis. Although a definitive conclusion will require computing the total dipole moment for the ion-molecule complex, the low polarizability of the lithium ion (the only aspect that is not included here), as compared with that of CCl_4, strongly suggests that the present conclusion will not change appreciably. The natural choice is then a model with point dipoles on each atomic site. The only available model is that proposed in Ref. 69 and used in MD simulations of the neat liquid and ionic solutions in Ref. 9 (see Sec. II B2 and Table IV). From the third panel in Fig. 5, we see that it is rather accurate for the *corner* configuration at all distances. This good degree of accord is reduced for the *edge* configuration and gets even poorer for the *face* configuration, so that the performance reduces for the most probable configurations. Also in Fig. 5 the results from a fluctuating charge model[84] are included. Its performance is almost identical to the five point dipole model that has been just discussed.

On the basis of the polarizability formulas for CCl_4 [Eqs. (9), (18), and (24)] we have optimized each method for the two most probable configurations (*face* and *edge*). Remarkably, no optimization of the fluctuating charge model is possible. From Eq. (9) we have that α_{CCl4} only depends on the difference $J_C^0 - J_{ClCl}$, so that these two parameters have to be increased or decreased proportionally, in order to keep the difference (and therefore the molecular polarizability) constant. Following this procedure, no changes are observed on the curves displayed in Fig. 5. Since this method fails particularly for the most probable configuration (*face*) we conclude that, as in the case of water, it has the worst performance and that, again, a more complex approach (with more point charges or mixed methods) is required in order to be comparable with the shell or point dipole methods. Together with the aforementioned difficulties for planar molecules and atomic ions, and despite its computational convenience, it seems fair to conclude that it should not be recommended as the method of choice if an accurate and fast calculation of induced dipoles is required.

Regarding the optimized shell and point dipoles methods, the results are displayed in Fig. 6. Parameters for the optimized shell model (SH-CCl4) are reported in Sec. II C, and those for the optimized point dipole (PD-CCl4) are given in Table IV. It can be seen that now they both satisfactorily reproduce the *ab initio* curves for the most probable configurations (*face* and *edge*), which highlights the importance of parameter optimization for each molecule in order to get the maximum performance, while at the same time keeping the behavior at long distances (molecular polarizability) intact. It is interesting to note that this optimization process, in the case of point dipoles, leads to a *negative* polarizability located on the carbon site (see parameters in Table IV). This possibility, which to our knowledge has never been considered before,[69] can be physically motivated if one considers that the main deficiency of the point dipole method lies in its inability to model intramolecular charge transfer. We see, as a result of the optimization process, that by using negative polarizabilities (for a *buried* atom), this approach is able to mimic alternating partial charges in a molecule that result from polarization by an ion. The fact that an ion often induces alternating changes in atomic partial charges if, for example, positioned on one end of a hydrocarbon molecule, is known since a long time. Semiempirical calculations that showed such results were among the first ones in coordina-

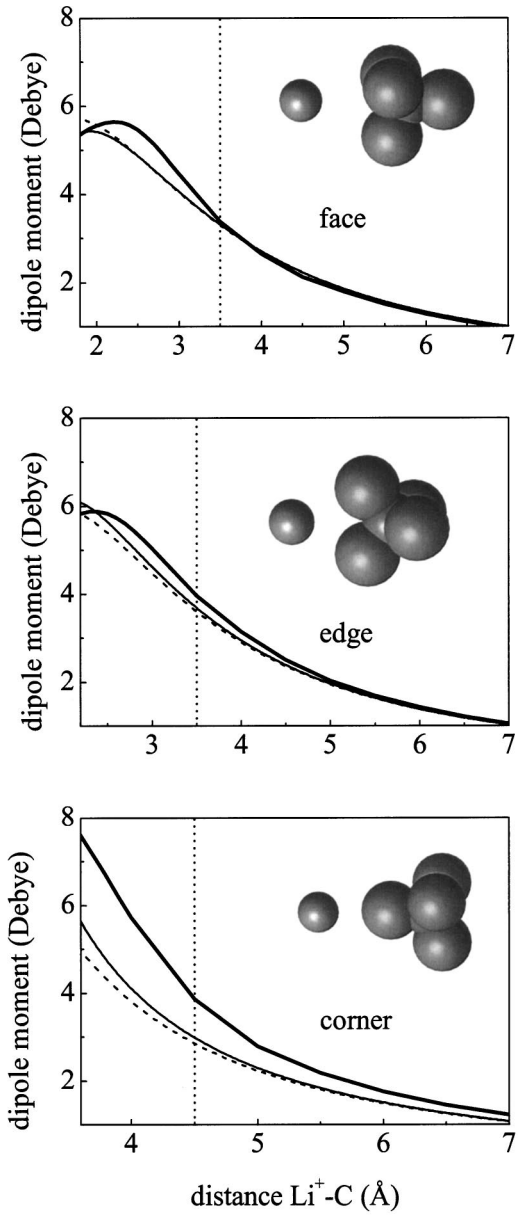

FIG. 6. CCl_4-monovalued charge: comparison of the best models. *Ab initio* (thick solid line), point dipole PD-CCl4 (thin solid line), and SH-CCl4 (dashed line).

tion chemistry.[100] Finally, for the less probable configuration (*corner*) both methods underestimate the induced dipole (by a ≈25% in the worst case). It is to be noted that this strong disagreement occurs for the configuration in which higher dipole moments are induced: for *face* and *edge* the maximum induced dipole is 6 D, while it goes up to almost 8 D for *corner*. As in the (much less pronounced) case of water close to lithium, where the *ab initio* curve is slightly above each method at intermediate distances, a likely explanation is that there are nonlinear polarization effects (with the consequent higher induced dipole in the *ab initio* calculation), which the classical methods are unable to reproduce. It is this particular issue that will be the focus of the following section.

V. MOLECULE CLOSE TO DIVALENT CHARGE

The models for water and for carbon tetrachloride that have been found to accurately reproduce the dipole moment close to a (point charge) lithium ion will be now tested in the environment of the (point charge) magnesium ion. No further optimization is now possible, any disagreement that may appear will signal unavoidable deficiencies of simple polarization methods, which would need to be addressed with *ad hoc* improvements.

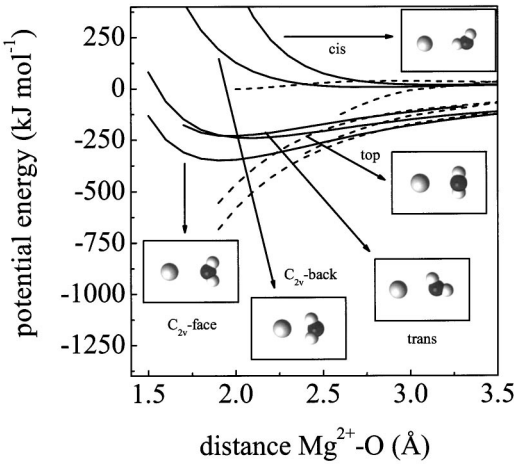

FIG. 7. *Ab initio* potential energy curves for Mg^{2+}-H_2O (solid lines) and for $(++)$-H_2O (dashed lines).

A. Water

A single point dipole located on a *M* site close to the oxygen or, to a lesser extent, a three point shell model, are the simplest models that accurately predict the induced dipole of a monovalued charge for all relevant distances (see Sec. IV). Only these two optimal methods will be now compared with the *ab initio* results for a divalent point charge. Figure 7 displays the Mg^{++}-H_2O energy profiles computed for several molecular orientations (full lines), together with the corresponding profiles for the point charge approximation (dashed lines). Qualitatively the results are very similar to those for the monovalent charge: C_{2v}-*face* is the most stable configuration (with the well depth increasing by about a factor of 2 with respect to the corresponding curve for Li^+), *top* and *trans* have similar but shallower attractive profiles, while *cis* and C_{2v}-*back* are dissociative. Concerning the accuracy of the point charge approximation it is virtually exact down to 3 Å for all configurations displayed in Fig. 7. The distance of maximum approach is of roughly 1.3 Å for C_{2v}-*face* and *trans* configurations, increases to ≈1.5 Å for *top* and, finally, is of about ≈2.3 Å for C_{2v}-*back*.

The results for the total dipole moment are displayed in Fig. 8. Each plot includes the *ab initio* result together with the best point dipole and shell models. Notice that in the case of the C_{2v}-*back* configuration the point dipole which is directed towards the ion at long separations, reverses its direction at ≈3.5 Å due to the contribution of the induced dipole, yielding negative values at shorter distances. Vertical dashed lines indicate the distance at which the potential energy profiles obtained for the ion or for a point charge are still indistinguishable. Although still not substantial, marked divergences already exist at these separations (where the point charge approximation for the ion is exact) between the

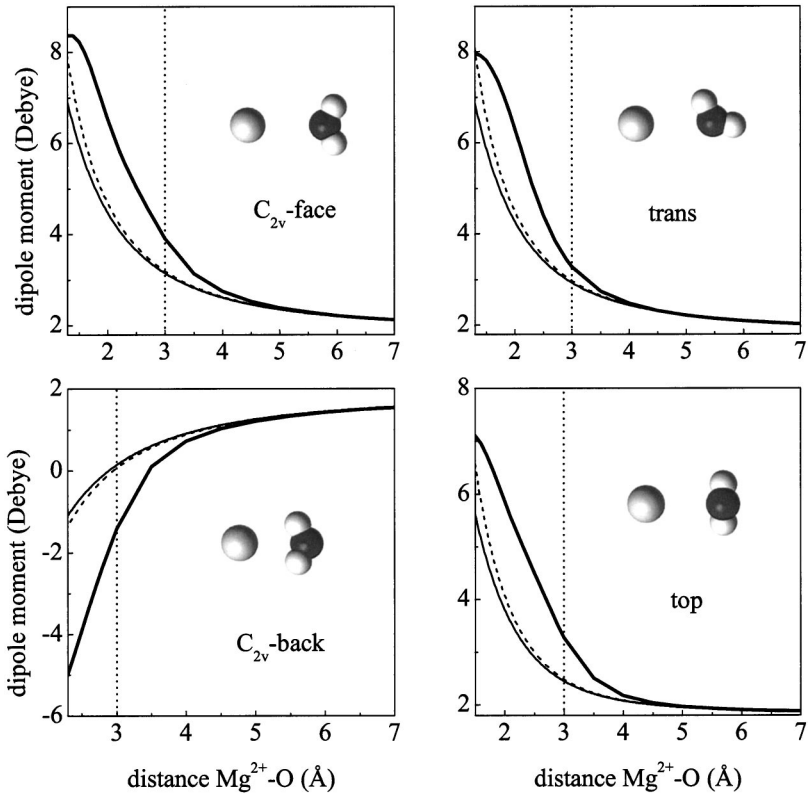

FIG. 8. Water-divalent charge: comparison of the best models. *Ab initio* (thick solid line), SH-H2O (thin solid line), and PDM (dashed line).

ab initio and classical polarization methods (themselves almost identical within all the range). These differences grow for smaller distances, although at the shortest separations the *ab initio* curves display a turnover (with a maximum of ≈8 D for the total dipole), which allows the classical methods to come closer again to the *ab initio* results (except for the C_{2v}-*back* configuration, due to a larger contact distance).

Regarding the interpretation of these results, we first note that for distances larger than 4–5 Å both methods provide highly accurate results, confirming the good performance of classical polarization methods for distances larger than about two molecular diameters (as observed for the Li^+-H_2O dimer). However, for smaller distances the performance is not as good as for the monovalent charge. The differences between classical and *ab initio* results can be rationalized as resulting from two sources, depending on the separation.

First, the underestimation of the induced dipole at ''intermediate'' separations (1.5–4 Å) should probably be ascribed to the lack of nonlinear contributions in the classical methods (hyperpolarizability), to a higher degree than what has already been observed in the analysis for the monovalent charge. Here the difference can go up to 2 D between the *ab initio* and classical curves (a substantial 50% in some cases, while for the *edge* configuration of the Li^+-CCl_4 dimer it was of about 30% in the worst case). Nonlinear effects can be better appreciated if we compare, for a fixed distance, the dipole induced by a monovalent charge with that induced by a divalent one. We take the case of the C_{2v}-*face* configuration for the ion-water dimer, with the distance fixed at 2 Å (that is, the most probable orientation close to the minimum of the corresponding potential energy profile, see Figs. 1 and 7). The total *ab initio* dipole for a lithium-water dimer is 3.57 D, i.e., an induced dipole moment of 1.72 D (given that water has a permanent dipole of 1.85 D). For the magnesium-water pair we get 6.53 D for the total *ab initio* dipole, i.e., and induced dipole of 4.68 D. The crucial point is that the latter is a factor 2.7 larger (compared to 1.72 D), while the charge has only increased by a factor of 2. If we now turn to the corresponding results obtained with the best classical model (PDM, which has one point dipole located at the *M* site), we find that the induced dipole is 1.4 D for the lithium-water dimer and 2.8 D for the magnesium-water dimer. Therefore, the induced dipole increases by exactly a factor of 2 when the charge is doubled, consistent with the expected linear behavior. In conclusion, it does not seem possible that any of the (linear) polarizable models studied is capable of reproducing the nonlinear increases with charge predicted by *ab initio* calculations.

Second, at separations close to contact the *ab initio* curves go through a maximum and slightly decrease at the closest separations, while the classical curves continue increasing. This damping that is here observed for the *ab initio* calculations supports the notion that a decrease of atomic polarizabilities at short distances should be expected due to the overlap of electronic charge distributions.[42] The better accord with the classical methods that is observed at contact is probably fortuituous, in the sense that polarization methods seem to perform better when they do not contain any mechanism to mimick electronic overlap. These results stem from two opposing trends: the underestimation at ''intermediate'' distances and the overestimation that can be expected at very short distances (in most cases classical methods tend to diverge for unphysically short separations). Put another

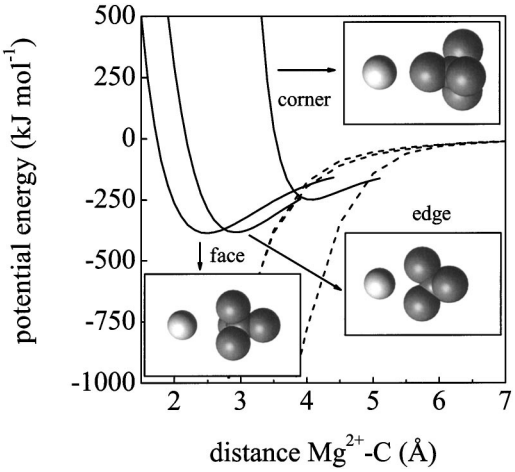

FIG. 9. *Ab initio* potential energy curves for Mg^{2+}-CCl_4 (solid lines) and for $(++)$-CCl_4 (dashed lines).

way, if the classical methods would have yielded a better accord at intermediate distances, then one should expect to find divergences at contact. In this connection, it is important to note that no divergences are found at contact separations even for this doubly charged ion, while they would probably appear in any method that would include nonlinear effects (which would require the use of damping schemes).

B. Carbon tetrachloride

Finally, we turn to CCl_4, for which it is to be expected that the features just discussed may become even more evident. Figure 9 displays the energy profiles computed for several molecular orientations (full lines), together with the corresponding profiles for the point charge approximation (dashed lines). Again, the qualitative results for the Mg^{++}-CCl_4 profiles are very similar to those for Li^+. The *face* and *edge* configurations have almost the same stability, albeit the well depth has increased by *more* than a factor of 3 (while the charge has only been doubled). The *edge* configuration also increases its well depth although, again, its position is located at a much larger distance and is therefore less probable. In contrast with all previous examples, there is a substantial disagreement with the point charge approximation for the ion (dashed lines) at all distances. Consequently, the comparison with *ab initio* results will only apply for the point charge-CCl_4 system. The distances of maximum approach barely change compared to those reported in Sec. IV B.

Figure 10 displays the results from the *ab initio* calculations together with those from the optimized point dipole (PD-CCl4) and shell (SH-CCl4) models (see Sec. IV B). The most remarkable aspect probably is the huge induced dipole moments predicted by the *ab initio* calculations, which go up to 25 D for the *edge* configuration. Certainly, these results correspond to the point charge-CCl_4 system and will have to await confirmation from a computation for the real Mg^{++}-CCl_4 dimer. Concerning the point that is of interest here, the comparison of the induced dipoles between *ab initio* and classical methods for a point charge, the basic results obtained for water are here reinforced. Basically, classical

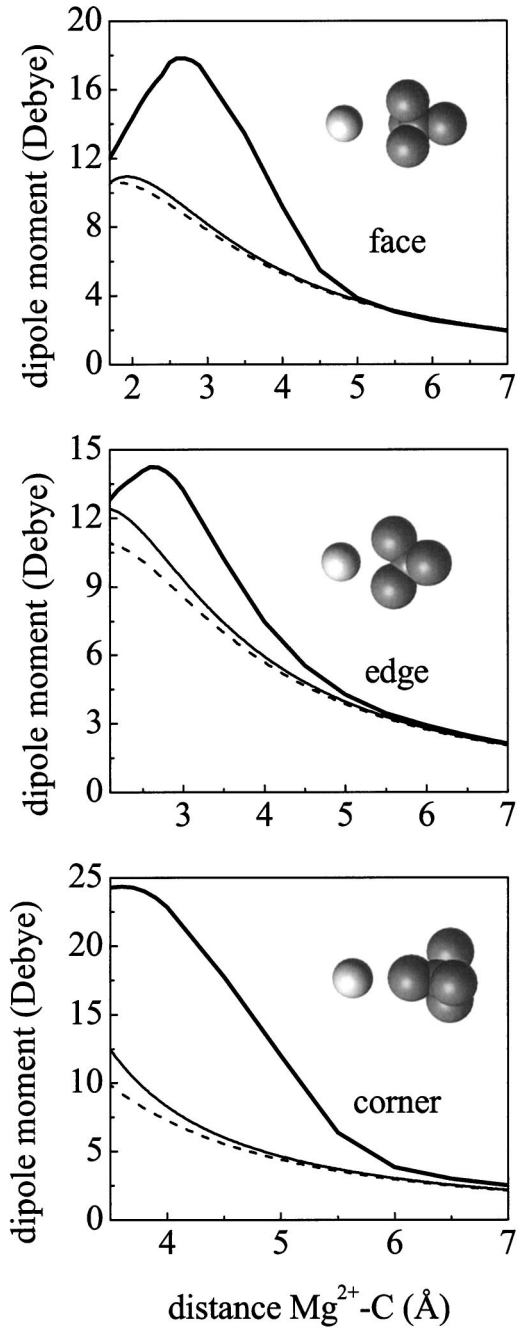

FIG. 10. CCl_4-divalent charge: comparison of the best models. *Ab initio* (solid bold line), PD-CCl4 (thin solid line), and SH-CCl4 (dashed line).

methods produce exact results for distances larger than one molecular diameter[101] ($\approx$5 Å), and underestimate the *ab initio* results for shorter distances. In this case the underestimation can be as large as a 50%. Again the *ab initio* results display a turnover for the closest distances, which in this case the classical methods are able to mimick to a certain extent. Again, there are no signs of divergence for the classical methods at contact separations, and no significant differences exist between point dipoles or shell models.

VI. CONCLUSIONS

To summarize, the point dipole or shell models are remarkably accurate at all distances in the vicinity of a small

monovalent charge. The analysis close to a divalent charge (or to a monovalent charge for highly polarizable molecules) suggests that the inclusion of hyperpolarizability might be required to cure the underestimation of the dipole moment at intermediate distances. It should be noted that in no case is damping required, so that the use of damping schemes based on divergences taking place during MD simulation of the liquid phase does not seem justified on physical grounds. Actually, in most configurations classical polarization methods tend to underestimate the induced dipole.

The present results discourage the use of the fluctuating charge method. Besides its known limitations for planar molecules and atomic ions, it has been shown that for carbon tetrachloride (a spherical molecule with five sites) it cannot describe, even if optimized, the induced dipole for the most probable molecular orientation. While a better performance might probably be obtained using a higher number of site charges, this solution is in conflict with the requirements of efficiency in MD simulations. In contrast, the point dipole and shell models display a high degree of flexibility, which has allowed to optimize their parameters and obtain a much better accord with *ab initio* calculations than would be possible by simply using transferable sets of parameters. In this sense, given the present feasibility of an ab initio analysis for each molecule of interest, it is probably advisable to perform a case per case parameter optimization instead of using reduced sets of atomic parameters which, although yielding acceptable results for a wide range of molecules, are not able to exploit the full capabilities of simple polarization methods. The example of the point dipole method applied to carbon tetrachloride illustrates this point: while it is improbable that a negative polarizability for the carbon atom is transferable, it is the one that yields the best accord with *ab initio* results for this particular molecule. Following this approach, and for the cases studied, the use of mixed methods does not seem necessary, specially considering that they do not seem to have the potential to reproduce nonlinear effects either.

Certainly, it is necessary to check whether the present conclusions hold for the real ion-molecule dimer and for this purpose the total induced dipole will be computed *ab initio* and with classical methods that include ion polarizability. No substantial changes are anticipated, though, given the low cation polarizability and the fact that the basic conclusions already hold in the region where the point charge approximation for the ion is highly accurate. Assuming that this is the case, schemes for including nonlinear effects will be studied. In this connection, although damping schemes seem not to be required in the cases studied here, if an additional nonlinear polarization is included, it might actually require the use of damping at contact. Finally, given the very good accord obtained with *ab initio* calculations for dimers in the gas phase, it seems essential to ascertain the possible variations of polarizability that may take place in condensed phase,[102–104] since at the present level of accuracy they may constitute the limiting factor in order to get a satisfactory representation of many-body effects in the condensed phase.

ACKNOWLEDGMENTS

This work was supported by EC TMR network HPRN-CT-2000-19 (''Solvation Dynamics and Ionic Mobility in Conventional and Polymer Solvents''), MCYT Project No. BFM2001-2077, and an Austria-Spain coordinated action.

APPENDIX: POLARIZATION TENSOR COMPONENTS

Here we outline the derivation of one of the polarization tensor components (α_{zz}) for the case of water. It should be reminded that the *z* axis is directed along the water symmetry axis, bisecting the angle between both oxygen-hydrogen stretches, with the origin located on the oxygen site (or the auxiliary site *M* characteristic of TIP models). Only the cases of fluctuating charges and point dipoles will be addressed, as the general expression for the shell method is already derived in Sec. II C.

1. Fluctuating charges

The molecular dipole moment in the *z* direction is given by $(q_{H_1}+q_{H_2})d\cos(\theta/2)$, where *d* denotes the O-H bond length and θ the bending angle. If the set of Eq. (4) is particularized for this case (only the equation for one of the two hydrogens is given), we obtain

$$\chi_H + J_H^0 q_{H_1} + J_{H_1H_2} q_{H_2} + J_{HO} q_O - d\cos(\theta/2)E = \chi, \quad \text{(A1)}$$

$$\chi_O + J_O^0 q_O + J_{HO} q_{H_1} + J_{HO} q_{H_2} = \chi, \quad \text{(A2)}$$

$$q_O + q_{H_1} + q_{H_2} = 0. \quad \text{(A3)}$$

Together with the fact that both hydrogens have the same charge ($q_{H_1}=q_{H_2}$), it is straightforward to obtain for the *induced* charge on each hydrogen,

$$q_H^{ind} = \frac{Ed\cos(\theta/2)}{J_H^0 + J_{H_1H_2} + 2J_O^0 - 4J_{HO}}. \quad \text{(A4)}$$

The induced dipole in the *z* direction is thus given by

$$p_z^{ind} = 2q_H^{ind} d\cos(\theta/2) = \frac{E2d^2\cos^2(\theta/2)}{J_H^0 + J_{H_1H_2} + 2J_O^0 - 4J_{HO}}, \quad \text{(A5)}$$

from which α_{zz} is readily identified[43] [see Eq. (8)].

2. Point dipoles

Under the effect of an external field in the *z* direction there are, in principle, nine induced dipole Cartesian components to be determined, which are reduced to only three due to symmetry considerations: the *z* component of the oxygen dipole moment (p_z^O), the *z* component of the hydrogen dipoles ($p_z^{H_1}$ and $p_z^{H_2}$, which will be equal), and possibly the *y* components of the hydrogen dipoles ($p_y^{H_1}$ and $p_y^{H_2}$, again equal in magnitude but of opposite signs).

We can compute, for instance, p_z^O expanding formula (14) and retaining terms different from zero:

$$p_z^O = \alpha_O[E + (T_{O\text{-}H_1})_{zz} p_z^{H_1} + (T_{O\text{-}H_1})_{zy} p_y^{H_1} + (T_{O\text{-}H_2})_{zz} p_z^{H_2} + (T_{O\text{-}H_2})_{zy} p_y^{H_2}] \quad \text{(A6)}$$

$$= \alpha_O\{E + [(T_{O\text{-}H_1})_{zz} + (T_{O\text{-}H_2})_{zz}]p_z^{H_1} + [(T_{O\text{-}H_1})_{zy} - (T_{O\text{-}H_2})_{zy}]p_y^{H_1}\}. \quad \text{(A7)}$$

From Eq. (12), the polarization tensor components are

$$(T_{O\text{-}H_1})_{zz} = (T_{O\text{-}H_2})_{zz} = \frac{1}{d^3}[3\cos^2(\theta) - 1], \quad \text{(A8)}$$

$$(T_{O\text{-}H_1})_{zy} = -(T_{O\text{-}H_2})_{zy} = \frac{3\cos(\theta)\sin(\theta)}{d^3}, \quad \text{(A9)}$$

which if inserted in the expression for p_z^O yield

$$p_z^O = \alpha_O\left[E + \frac{2}{d^3}[3\cos^2(\theta) - 1]p_z^{H_1} + \frac{6\cos(\theta)\sin(\theta)}{d^3}p_y^{H_1}\right]. \quad \text{(A10)}$$

In a similar way corresponding expressions can be derived for the other two components:

$$p_z^{H_1} = \alpha_H\left[E + \frac{3\cos^2(\theta) - 1}{d^3}p_z^O - \frac{1}{8d^3\sin^3(\theta)}p_z^{H_1}\right], \quad \text{(A11)}$$

$$p_y^{H_1} = \alpha_H\left[\frac{3\cos(\theta)\sin(\theta)}{d^3}p_z^O - \frac{1}{4d^3\sin^3(\theta)}p_y^{H_1}\right]. \quad \text{(A12)}$$

From the last three equations it is straightforward to express the dipole components in terms of E. When inserted in the expression for the total dipole moment ($p_z = p_z^O + 2p_z^{H_1}$), α_{zz} is readily identified [see Eq. (17)].

[1] A. van der Vaart, B. D. Bursulaya, C. L. Brooks, and K. K. Merz, J. Phys. Chem. B **104**, 9554 (2000).
[2] T. A. Halgren and W. Damm, Curr. Opin. Struct. Biol. **11**, 236 (2001).
[3] S. Patel and C. L. Brooks, J. Comput. Chem. **25**, 1 (2004).
[4] P. Cieplak, J. Caldwell, and P. Kollman, J. Comput. Chem. **22**, 1048 (2001).
[5] L. X. Dang, J. E. Rice, J. Caldwell, and P. A. Kollman, J. Am. Chem. Soc. **113**, 2481 (1991).
[6] L. X. Dang and D. E. Smith, J. Chem. Phys. **99**, 6950 (1993).
[7] W. L. Jorgensen and D. L. Severance, J. Chem. Phys. **99**, 4233 (1993).
[8] D. E. Smith and L. X. Dang, J. Chem. Phys. **100**, 3757 (1994).
[9] T. M. Chang, K. A. Peterson, and L. X. Dang, J. Chem. Phys. **103**, 7502 (1995).
[10] S. J. Stuart and B. J. Berne, J. Phys. Chem. **100**, 11934 (1996).
[11] M. A. Carignano, G. Karlström, and P. Linse, J. Phys. Chem. B **101**, 1142 (1997).
[12] T. M. Chang and L. X. Dang, J. Phys. Chem. B **101**, 10518 (1997).
[13] A. A. Chialvo, P. T. Cummings, J. M. Simonson, and R. E. Mesmer, Fluid Phase Equilib. **150–151**, 107 (1998).
[14] L. X. Dang, J. Chem. Phys. **113**, 266 (2000).
[15] S. Nagakawa, J. Phys. Chem. A **104**, 5281 (2000).
[16] G. H. Peslherbe, B. M. Ladanyi, and J. T. Hynes, J. Phys. Chem. A **104**, 4533 (2000).
[17] J. M. Martínez, J. Hernández-Cobos, H. Saint-Martin, R. R. Pappalardo, I. Ortega-Blake, and E. Sánchez Marcos, J. Chem. Phys. **112**, 2339 (2000).
[18] S. Koneshan, J. C. Rasaiah, and L. X. Dang, J. Chem. Phys. **114**, 7544 (2001).
[19] R. Ayala, J. M. Martínez, R. R. Pappalardo, H. Saint-Martin, I. Ortega-Blake, and E. Sánchez Marcos, J. Chem. Phys. **117**, 10512 (2002).
[20] R. Fischer, J. Richardi, P. H. Fries, and H. Krienke, J. Chem. Phys. **117**, 8467 (2002).
[21] E. Oyen and R. Hentschke, Langmuir **18**, 547 (2002).
[22] M. Kubo, R. M. Levy, P. J. Rossky, N. Matubayasi, and M. Nakahara, J. Phys. Chem. B **106**, 3979 (2002).
[23] R. Ayala, J. M. Martínez, R. R. Pappalardo, and E. Sánchez Marcos, J. Chem. Phys. **119**, 9538 (2003).
[24] M. Carrillo-Tripp, J. Saint-Martin, and I. Ortega-Blake, J. Chem. Phys. **118**, 7062 (2003).
[25] A. Grossfield, P. Ren, and J. W. Ponder, J. Am. Chem. Soc. **125**, 15671 (2003).
[26] T. V. Nguyen and G. H. Peslherbe, J. Phys. Chem. A **107**, 1540 (2003).
[27] S. Yoo, Y. A. Lei, and X. C. Zeng, J. Chem. Phys. **119**, 6083 (2003).
[28] M. J. Elrod and R. J. Saykally, Chem. Rev. (Washington, D.C.) **94**, 1975 (1994).
[29] P. Barnes, J. L. Finney, J. D. Nicholas, and J. E. Quinn, Nature (London) **282**, 459 (1979).
[30] P. Alström, A. Wallqvist, S. Engström, and B. Jönsson, Mol. Phys. **68**, 563 (1989).
[31] A. Wallquist, P. Alström, and G. Karlström, J. Phys. Chem. **94**, 1649 (1990).
[32] U. Niesar, G. Corongiu, E. Clementi, G. R. Kneller, and D. K. Bhattacharya, J. Phys. Chem. **94**, 7949 (1990).
[33] J. Caldwell, L. X. Dang, and P. A. Kollman, J. Am. Chem. Soc. **112**, 9144 (1990).
[34] H. Saint-Martin, C. Medina-Llanos, and I. Ortega-Blake, J. Chem. Phys. **93**, 6448 (1990).
[35] M. Sprik, J. Phys. Chem. **95**, 2283 (1991).
[36] S. B. Zhu, S. Singh, and G. W. Robinson, J. Chem. Phys. **95**, 2791 (1991).
[37] C. Millot and A. J. Stone, Mol. Phys. **77**, 439 (1992).
[38] L. X. Dang, J. Chem. Phys. **97**, 2659 (1992).
[39] R. E. Kozack and P. C. Jordan, J. Chem. Phys. **96**, 3120 (1992).
[40] A. Wallqvist and B. J. Berne, J. Phys. Chem. **97**, 13841 (1993).
[41] J. W. Halley, J. R. Rustad, and A. Rahman, J. Chem. Phys. **98**, 4110 (1993).
[42] D. N. Bernardo, Y. Ding, K. Krogh-Jespersen, and R. M. Levy, J. Phys. Chem. **98**, 4180 (1994).
[43] S. W. Rick, S. J. Stuart, and B. J. Berne, J. Chem. Phys. **101**, 6141 (1994).
[44] B. J. Palmer, Chem. Phys. **184**, 163 (1994).
[45] D. Borgis and A. Staib, Chem. Phys. Lett. **238**, 187 (1995).
[46] J. C. Soetens and C. Millot, Chem. Phys. Lett. **235**, 22 (1995).
[47] A. A. Chialvo and P. T. Cummings, J. Chem. Phys. **105**, 8274 (1996).
[48] L. X. Dang and T. M. Chang, J. Chem. Phys. **106**, 8149 (1997).
[49] B. Chen, J. Xing, and J. I. Siepmann, J. Phys. Chem. B **104**, 2391 (2000).
[50] H. Saint-Martin, J. Hernández-Cobos, M. I. Bernal-Uruchurtu, I. Ortega-Blake, and H. J. C. Berendsen, J. Chem. Phys. **113**, 10899 (2000).
[51] B. Guillot and Y. Guissani, J. Chem. Phys. **114**, 6720 (2001).
[52] G. Ferenczy and C. A. Reynolds, J. Phys. Chem. A **105**, 11470 (2001).
[53] H. A. Stern, F. Rittner, B. J. Berne, and R. A. Friesner, J. Chem. Phys. **115**, 2237 (2001).
[54] K. H. Cho, K. T. No, and H. A. Scheraga, J. Mol. Struct. **641**, 77 (2002).
[55] C. J. Burnham and S. S. Xantheas, J. Chem. Phys. **116**, 5115 (2002).
[56] H. Yu, T. Hansson, and W. F. van Gunsteren, J. Chem. Phys. **118**, 221 (2003).
[57] P. Ren and J. W. Ponder, J. Phys. Chem. B **107**, 5933 (2003).
[58] G. Lamoreoux and B. Roux, J. Chem. Phys. **119**, 3025 (2003).
[59] E. M. Mas, J. Chem. Phys. **118**, 4386 (2003).
[60] G. A. Kaminski, R. A. Friesner, and R. Zhou, J. Comput. Chem. **24**, 267 (2003).
[61] Z. Z. Yang, Y. Wu, and D. X. Zhao, J. Chem. Phys. **120**, 2541 (2004).
[62] E. M. Yezdimer and P. T. Cummings, Mol. Phys. **97**, 993 (1999).
[63] B. Chen, J. Xing, and J. I. Siepmann, J. Phys. Chem. B **104**, 2391 (2000).
[64] M. Predota, A. A. Chialvo, and P. T. Cummings, Fluid Phase Equilib. **183–184**, 295 (2001).
[65] H. J. C. Berendsen, J. R. Grigera, and T. P. Straatsma, J. Phys. Chem. **91**, 6269 (1987).
[66] W. L. Jorgensen, J. Chandrasekar, J. D. Madura, R. W. Impey, and M. L. Klein, J. Chem. Phys. **79**, 926 (1983).
[67] M. Alfredsson, J. P. Brodholt, K. Hermansson, and R. Vallauri, Mol. Phys. **94**, 873 (1998).
[68] I. Alkorta, M. Bachs, and J. J. Pérez, Chem. Phys. Lett. **224**, 160 (1994).

[69] J. Applequist, J. R. Carl, and K. K. Fung, J. Am. Chem. Soc. **94**, 2952 (1972).
[70] B. T. Thole, Chem. Phys. **59**, 341 (1981).
[71] R. R. Birge, J. Chem. Phys. **72**, 5312 (1980).
[72] A. K. Rappé and W. A. Goddard III, J. Phys. Chem. **95**, 3358 (1991).
[73] P. Drude, *The Theory of Optics* (Longmans, Green, New York, 1902), translation by C. Riborg Mann and R. A. Millikan.
[74] H. H. Loeffler, J. Comput. Chem. **24**, 1232 (2003).
[75] R. Armunanto, C. F. Schwenk, and B. M. Rode, J. Phys. Chem. A **107**, 3132 (2003).
[76] D. Spangberg and K. Hermansson, J. Chem. Phys. **120**, 4829 (2004).
[77] B. T. Thole and P. T. Van Duijnen, Chem. Phys. **72**, 211 (1982); Theor. Chim. Acta **55**, 307 (1980); P. T. Van Duijnen and J. A. C. Rullmann, Int. J. Quantum Chem. **38**, 181 (1990).
[78] A. J. Stone, Mol. Phys. **56**, 1065 (1985).
[79] U. Dinur, J. Phys. Chem. **97**, 7894 (1993).
[80] H. A. Stern, G. A. Kaminski, J. L. Banks, R. Zhou, B. J. Berne, and R. A. Friesner, J. Phys. Chem. B **103**, 4730 (1999).
[81] G. A. Kaminski, H. A. Stern, B. J. Berne, R. A. Friesner, Y. X. X. Cao, R. B. Murphy, R. H. Zhou, and T. A. Halgren, J. Comput. Chem. **23**, 1515 (2002).
[82] E. L. Sibert III and R. Rey, J. Chem. Phys. **116**, 237 (2002).
[83] R. Chelli, S. Ciabatti, G. Cardini, R. Righini, and P. Procacci, J. Chem. Phys. **111**, 4218 (1999).
[84] E. Llanta and R. Rey, Chem. Phys. Lett. **340**, 173 (2001).
[85] E. Llanta, K. Ando, and R. Rey, J. Phys. Chem. B **105**, 7783 (2001).
[86] C. J. F. Böttcher, *Theory of Electric Polarisation*, 2nd ed. (Elsevier, New York, 1973).
[87] D. van Belle, M. Froeyen, G. Lippens, and S. J. Wodak, Mol. Phys. **77**, 239 (1992).
[88] A. J. Cohen and Y. Tantirungrotechai, Chem. Phys. Lett. **299**, 465 (1999).
[89] P. Hohenberg and W. Kohn, Phys. Rev. **136**, B864 (1964); S. H. Vosko, L. Wilk, and M. Nusair, Can. J. Phys. **58**, 1200 (1980).
[90] A. D. Becke, Phys. Rev. A **38**, 3098 (1988); C. Lee, W. Yang, and R. G. Parr, Phys. Rev. B **37**, 785 (1988).
[91] A. D. Becke, J. Chem. Phys. **98**, 5648 (1993).
[92] P. Fuentalba and Y. Simn-Manso, J. Phys. Chem. A **101**, 4231 (1997).
[93] D. J. Tozer and N. C. Handy, J. Chem. Phys. **109**, 10180 (1998).
[94] J. P. Perdew, K. Burke, and M. Ernzerhof, Phys. Rev. Lett. **77**, 3865 (1996).
[95] A. J. Sadlej, Theor. Chim. Acta **79**, 123 (1992).
[96] D. E. Woon and T. H. Dunning, Jr., J. Chem. Phys. **98**, 1358 (1993); K. A. Peterson, D. E. Woon, and T. H. Dunning, Jr., *ibid.* **100**, 7410 (1994).
[97] W. Koch and M. C. Holthausen, *A Chemist's Guide to DFT* (Wiley-VCH, Weinheim, 2001), p. 178.
[98] A. D. McLean and G. S. Chandler, J. Chem. Phys. **72**, 5639 (1980).
[99] M. Masia and R. Rey, J. Phys. Chem. B **107**, 2651 (2003).
[100] V. Gutmann, *The Donor-Acceptor Approach to Molecular Interactions* (Plenum, New York, 1978).
[101] R. Rey, L. C. Pardo, E. Llanta, K. Ando, D. O. López, J. L. Tamarit, and M. Barrio, J. Chem. Phys. **112**, 7505 (2000).
[102] A. Morita and S. Kato, J. Chem. Phys. **110**, 11987 (1999).
[103] A. Morita, J. Comput. Chem. **23**, 1466 (2002).
[104] T. J. Giese and D. M. York, J. Chem. Phys. **120**, 9903 (2004).